GaAs-based self-aligned stripe superluminescent diodes processed normal to the cleaved facet

O M S Ghazal[a], D. Lei[a], D T Childs[b], B J Stevens[a], N Babazadeh[b], R A Hogg[b], and K M Groom[a]
[a] Department of Electronic & Electrical Engineering, The University of Sheffield, Nanoscience & Technology Building, North Campus, Broad Lane, Sheffield, S3 7HQ, United Kingdom; [b] Now at School of Engineering, The University of Glasgow, Rankine Building, Glasgow, G12 8LT UK

ABSTRACT

We demonstrate GaAs-based superluminescent diodes (SLDs) incorporating a window-like back facet in a self-aligned stripe. SLDs are realised with low spectral modulation depth (SMD) at high power spectral density, without application of anti-reflection coatings. Such application of a window-like facet reduces effective facet reflectivity in a broadband manner. We demonstrate 30mW output power in a narrow bandwidth with only 5% SMD, outline the design criteria for high power and low SMD, and describe the deviation from a linear dependence of SMD on output power as a result of Joule heating in SLDs under continuous wave current injection. Furthermore, SLDs processed normal to the facet demonstrate output powers as high as 20mW, offering improvements in beam quality, ease of packaging and use of real estate.

Keywords: superluminescent diode

INTRODUCTION

Superluminescent diodes (SLDs) offer relatively high power over a broad and smooth emission spectrum. Their waveguide structure enables far higher brightness than light emitting diodes (LEDs) and efficient fibre coupling, useful in many applications such as fibre-optic gyroscopes and optical coherence tomography (OCT). Biological applications require light penetration into highly turbid and absorbing tissue, with the range of near-IR wavelengths accessed by GaAs based devices being ideally suited to this biological band [7]. A key parameter used to define the coherence properties of the SLD is the spectral modulation depth, or ripple, which occurs due to parasitic Fabry-Perot resonances arising from non-zero reflection at the facets of the device. Current methods to suppress such reflections rely on the use of anti-reflection (AR) coatings, tilted facets, or a combination of the two. AR coatings directly decrease the facet reflectivity, however, is difficult to achieve ultra-low facet reflectivity over broad bandwidths. This is problematic for present requirements of ~100nm bandwidth and will become more so as broader band materials are developed (with hundreds of nm desirable for biological applications). By mis-orienting waveguides to the crystal-axis by an angle (typically 5 to 10°) from the normal to the cleaved facet, tilted facets suppress back reflection from the facet by deflecting reflected light outside the waveguide. This allows an effective facet reflectivity, R_{eff}, (which defines the amount of light that is coupled back into the waveguide) as low as ~10^{-4}, which can be further reduced to ~10^{-5} when combined with an AR coating [1].

Transparent (window) regions can provide typical R_{eff} <10^{-3} [2]. In a traditional window structure, the waveguide is terminated and light is allowed to spread in an un-pumped region prior to the cleaved facet such that only a small fraction of the light is re-coupled back into the waveguide following reflection at the cleaved facet. Windows are inherently broad-band and can be further combined with AR coatings and tilted waveguides to offer R_{eff} below 10^{-5} [3]. Furthermore, the use of absorbing sections to reduce R_{eff} below 10^{-6} has been shown, using bent passive absorbers [4,5], or grounded absorbers [6]. With respect to ridge waveguide approaches, buried ridge or stripe methods allow for narrow active widths and control of carrier flow, reduced non-radiative recombination at exposed surfaces, and greater control of the optical beam profile allowing for improved coupling to fibre.

Typically, GaAs-based SLDs are realised using a combination of AR coatings and tilted facets. In addition, etched deflectors and long tapered absorbers have been demonstrated [8]. However, a limited number of reports have been made on window facets. Although commonplace on InP [9], it is difficult to transfer to GaAs due to the requirement for regrowth upon exposed aluminium-containing layers. Window facets on GaAs have mainly been limited to the creation of non-interacting facets for raising the catastrophic optical damage (COD) threshold in high-power lasers [10], and processes where aluminium-containing layers are exposed prior to overgrowth of the transparent window are typically reported [11,12]. Such processes raise concerns over the long-term reliability of a growth interface on oxidised AlGaAs. Furthermore, alternative solutions comprising GaInP cladding lack design flexibility due to the limited range for which the refractive index can be tailored whilst retaining virtual lattice match and the smaller conduction band offset compared to AlGaAs cladding. In this paper we present a scheme for low R_{eff} facets, based on the application of a self-aligned stripe regrowth process [13], to realise window-like structures in GaAs-based SLDs. We demonstrate low spectral modulation depth (SMD) from SLDs with no facet coating, making them naturally broadband, and demonstrate that the ultra-low R_{eff} in these structures can allow SLDs to be processed without mis-orientating to the crystal axis (ie. with a normal-to-facet waveguide).

Our self-aligned stripe technology consists of a two-stage growth sequence in which GaAs/AlGaAs cladding layers are regrown upon a patterned GaInP optoelectronic confinement layer to form the cross-section shown schematically in Fig. 1, which provides both optical and electrical confinement. By terminating the waveguide prior to the cleaved facet, as shown in the cross-section along the waveguide in Fig.1 (b), light is allowed to spread out in the laterally unguided window region. However, in contrast to traditional optically transparent window structures, the active region remains intact, forming a window-like region. In this region, situated below the opto-electronic confining GaInP layer, light also undergoes absorption resulting in further suppression of feedback into the waveguide and correspondingly lower R_{eff}. A simple calculation of the contrast between the modal refractive index in the stripe (3.284) and in the window region (3.281) using Snell's law suggests R_{eff} ~10^{-7}, applying for a plane wave incident upon an abrupt interface. However, the real interface is not abrupt due to the angled regrowth interface resulting from the GaInP wet etch, which is expected to reduce this effective reflectivity. Measurements described elsewhere indicate $R_{eff} < 10^{-7}$ for 1mm long windows aligned to the crystal axis (normal-to-facet), further reduced through mis-orienting the waveguide, or application of an AR coating.

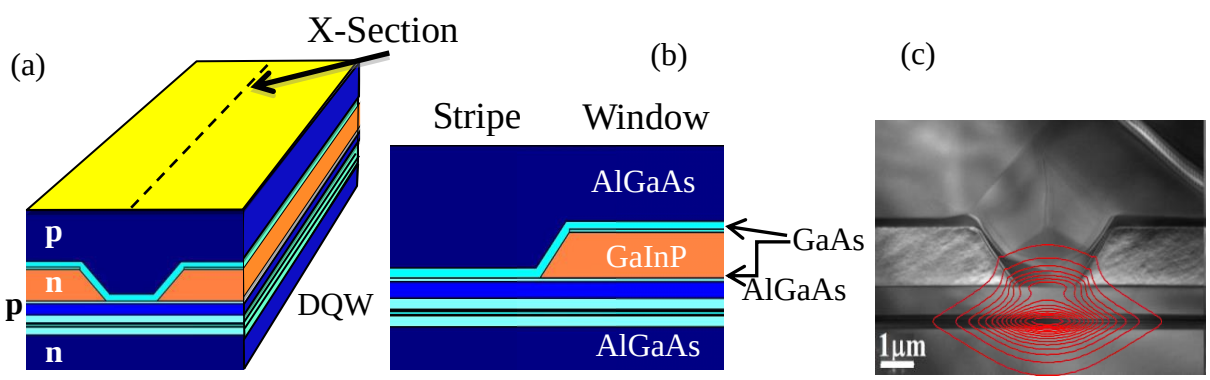

Figure 1. (a) Schematic diagram of our self-aligned stripe. A cross-section along the stripe, shown by the dotted line in (a), is shown in (b) about the active-window interface. A transmission electron micrograph (TEM) is shown in (c), taken through the active stripe of this device. A simulated optical mode profile is overlaid upon the TEM to illustration its position within the structure.

SAMPLE PREPARATION

A waveguide structure was grown based on that described previously [13], containing two 7.6nm $In_{0.17}Ga_{0.83}As$ QWs separated by 10nm $GaAs_{0.9}P_{0.1}$ strain balancing layers, and 50nm GaAs at either side forming the waveguide core. This core was grown within n-doped $Al_{0.42}Ga_{0.58}As$ lower cladding and 300nm p-doped $Al_{0.42}Ga_{0.58}As$. 20nm GaAs was

grown prior to 600nm n-doped GaInP, lattice matched to GaAs, and finally 15nm GaAs. Self-aligned stripes were patterned using standard photolithography (oriented 10° off from the normal to the crystal axis in one half of the wafer and aligned to the crystal axis in the other) and etched via a combination of dry and highly selective wet chemical etching using H_3PO_4/HCl, which stops abruptly at the GaAs layer immediately below the GaInP layer. Samples were cleaned and returned to the MOVPE reactor for overgrowth of 100nm p-doped GaAs, 1500nm p-doped $Al_{0.42}GaAs$, and 200nm p-doped GaAs. Following growth, electrical isolation trenches were etched down to the GaInP layer at either side of the stripe, continuing throughout the entire length of the structure in order to create 100µm wide electrically isolated devices. Au/Zn/Au ohmic contacts were applied above the stripe before a SiN layer was deposited and a window etched above the stripe to allow application of TiAu bondpads. These were deposited, then the substrate was thinned and a back InGe/Au contact applied. Cleaved SLDs were mounted epi-side down with a AuSn-containing paste upon AlN tiles, and tested at room temperature.

RESULTS I – TILTED FACET

In order to demonstrate the relative performance of SLDs with different stripe geometries, 3 SLDs are compared in Figure 2. The SLDs shown have the following stripe lengths (all 3µm wide): 1mm with 1mm window, 1.7mm with 0.7mm window, and 3mm with 2mm window. At these long window lengths, window length was shown not to be a significant factor (from a comparison of 1.7mm long SLD with different window length). Fig. 2 (a) plots the output power as a function of current density for the 3 SLDs. Lasing is suppressed up to the maximum powers shown (as examined in high-resolution spectra not shown here).

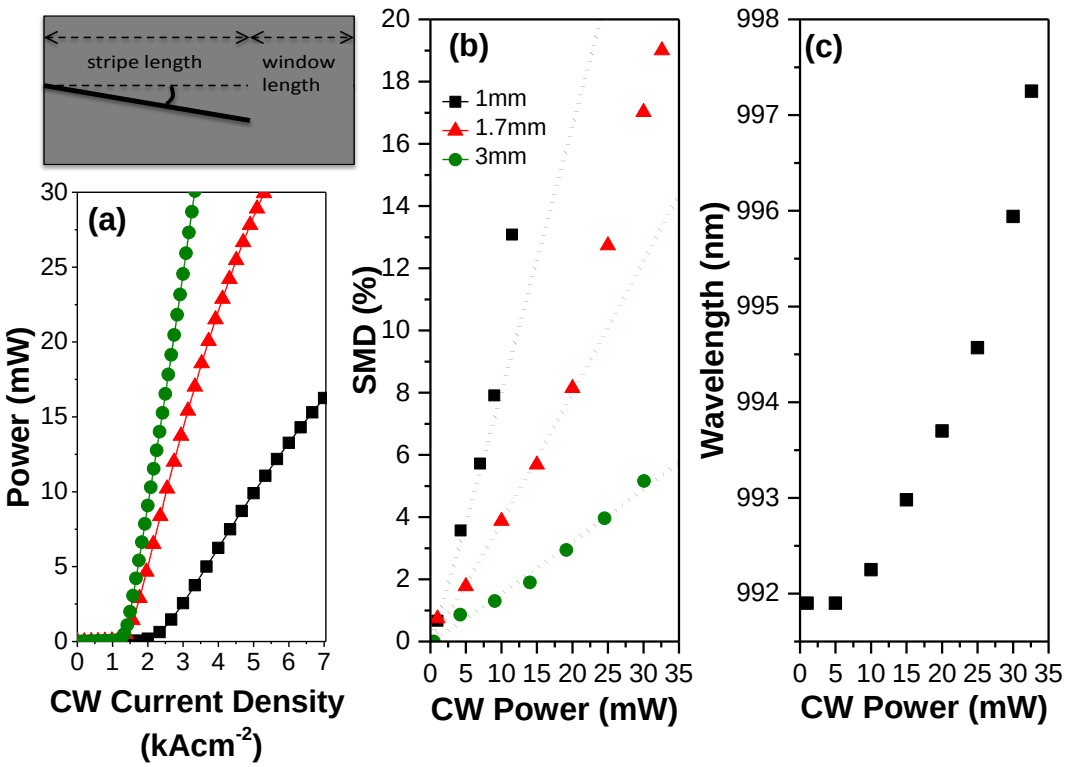

Figure 2. (a) Power as a function of current density for SLDs with 4 different geometries, (b) SMD vs power for the four devices. The dotted lines represent a fit to the experimental data. (c) plots the peak wavelength as a function of CW output power.

High resolution electroluminescence (EL) spectra were recorded using an Advantest Q8384 optical spectrum analyzer with 0.01nm resolution. A mode spacing of 0.08nm allows accurate determination of the peak and valley intensities

within the spectrum. This mode spacing is consistent with the length of the active stripe, corresponding to reflection at the stripe/window interface. A plot of SMD as a function of output power is constructed in Figure 2 (b), together with fits to the data as shown by the dotted lines. The SMD is seen to increase with increasing power for all stripe lengths, with a smaller gradient for larger stripe lengths. It is possible to fit the data only at low current. However, at high current, an abrupt deviation occurs. We attribute this deviation to Joule heating in the SLDs, which are pumped using a continuous wave (CW) current source. Figure 2 (c) plots the evolution of the EL spectrum of the 1.7mm long SLD, recorded at a lower resolution of 0.1nm from 1mW to 30mW. At high current densities the central wavelength of the emission spectrum is observed to red-shift by ~6nm when ~6kAcm^{-2} is injected.

Absorption in the window-like region of our SLD is beneficial in attaining such low R_{eff}. Surface aperture mesa diodes were fabricated in order to investigate the absorption spectrum through measurement of the photocurrent spectrum. By scanning the IR light emitted by a tungsten halogen bulb through a monochromator and impinging this upon the mesa, the photocurrent spectrum can be plotted. This is shown in Figure 3 (a), exhibiting a peak centred at 992nm, coinciding with the central wavelength of emission at low current densities. Therefore, at low current densities (corresponding to low output powers) light travelling from the active stripe through the window region will be absorbed, contributing to the very low SMD. As observed in Fig. 3 (c), at higher current densities self-heating in the active stripe results in a red-shift of emission by 6nm between output powers of 1 and 32.6mW from the 1.7mm long SLD. Meanwhile, non-ideal heat spreading in the buried stripe means that the unpumped window region probably operates at a cooler temperature, and the SLD emission peak shifts to the longer side of the absorption peak. The lower absorption available at these longer wavelengths may therefore permit light to travel through the window, which becomes increasingly transparent with increasing current density. This mechanism can be linked back to the behavior observed in Fig. 3 (b), in which two fits are necessary to the SMD versus power curve for the SLD with 1.7mm stripe length, with differing rear facet R_{eff} – one for powers <20mW and another for powers >20mW. Below 20mW the central emission wavelength is still coincident with the absorption peak in the window, while at higher powers the central wavelength is red-shifted to about 998.5nm where the absorption is clearly reduced.

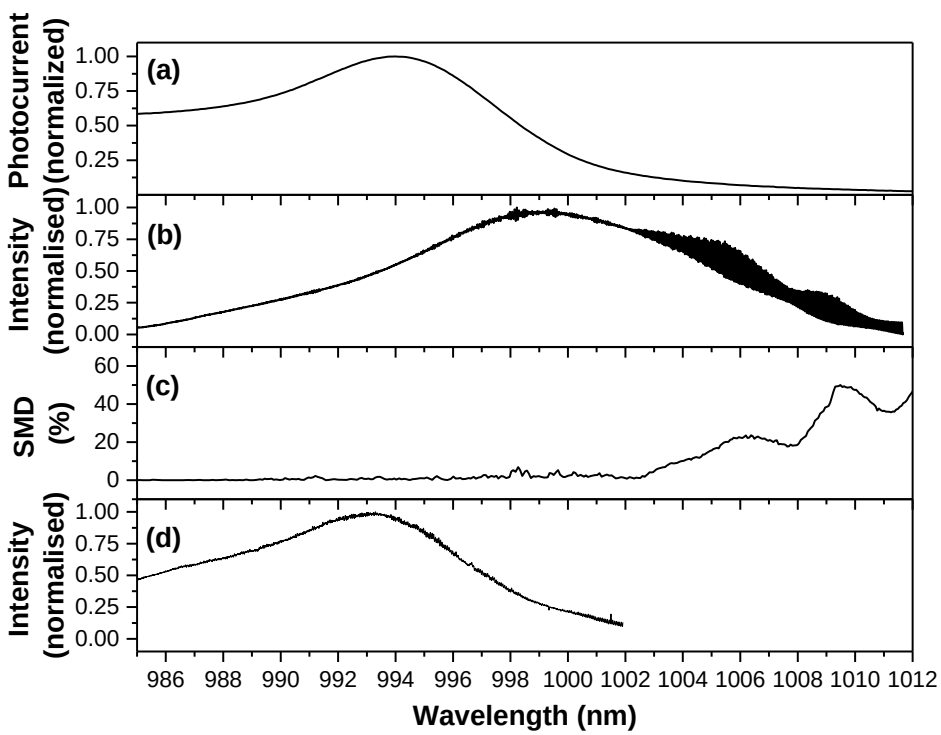

Figure 3. (a) Photocurrent spectrum used to describe the absorption in the window region. (b) High-resolution EL spectrum of 1mm long SLD at 10kAcm-2 (23.2mW) and corresponding plot of SMD across this spectrum in (c), demonstrating larger SMD to longer wavelengths.(d) Pulsed (10μs, 1ms) EL spectrum at 38mW exhibit <1nm red-shift with respect to its absorption peak and <2% SMD.

Fig. 3 (b) plots the high-resolution EL spectrum, with the corresponding spectral dependence of the SMD extracted for the 1.7mm long SLD at maximum power in Fig 3 (c). SMD >20% is observed beyond ~1000nm, compared to <5% at shorter wavelengths, for identical spectral mode power. Since these thermal effects are a manifestation of self-heating in the self-aligned stripe, it could be assumed that operation in a pulsed regime would suppress the red-shift and result in lower SMD to higher powers, in the absence of self-heating. This would present the case when efficient heat-sinking is applied to the CW SLD. Figure 3 (d) plots the high-resolution EL spectrum recorded under pulsed current injection (10μs pulse width and 1% duty cycle) for the 1.7mm long SLD, at an output of 38mW (normalized to CW). Negligible red-shift (<1nm) is observed up to this maximum power, resulting in SMD ~1-2%, confirming our assumptions about the origin of the high SMD in our very high power devices.

RESULTS II – NORMAL-TO-FACET

Such a high level of feedback suppression should allow waveguides to be processed parallel to the crystal axis. Using such normal-to-facet approaches offers two main advantages over mis-oriented waveguides (tilted facets) with regards to component manufacture and packaging. First, narrower chip widths can be obtained down to the limits of cleaving (~3 × substrate thickness) compared with the wider chip size for tilted facet SLDs, as defined by trigonometry. This means more components can be diced from a wafer. Second, beam quality is improved for the normal facet compared with the crescent shaped output expected from the tilted facet. Furthermore, mounting in standard mounts becomes easier for normal waveguides.

Normal-to-facet SLDs were processed from identical material to that used for the tilted facet SLDs above, albeit with overgrowth performed in a separate run. Following fabrication of self-aligned stripe window-facet SLDs with a range of stripe widths, the cleaved output facet of these devices was coated with a simple, single $\lambda/4n$ SiN coating using plasma enhanced chemical vapour deposition (PECVD). The role of this coating is to decrease the reflectivity of the output facet so as to allow light to escape from the device, which would otherwise be subject to 30% reflection at the semiconductor/air interface. In case of such reflectivity carrier depletion resulting from photons propagating in the opposite direction along the stripe reduces the power generated in the output direction, resulting in lower output power. SLDs were cleaved with stripe lengths of 0.5, 1, and 2mm and with 1mm long window regions, and mounted epi-side up on alumina tiles for testing at room temperature using a CW current source.

The performance of 1mm long SLDs with 1mm windows can be described using Fig 4. Fig 4 (a) plots the power as a function of CW current for 5, 7 and 10μm wide stripes. Output power >20mW was recorded for all three stripe widths, with efficiency greater for the wider stripes, which offer more gain due to higher coupling between the optical mode and the QWs. Fig 4 (b) plots the EL spectra for the three SLDs at an output power of 20mW, recorded at low resolution (0.1nm) under CW injection. The wider stripe undergoes an expected shift to longer wavelength whilst the narrower stripes also undergo spectral broadening to shorter wavelengths, attributed to state-filling as also observed in shorter length SLDs. Importantly, the SLDs do not show evidence for lasing. The corresponding high resolution (0.01nm) spectrum is plotted for the 10μm wide SLD in Fig 4 (c) at the central wavelength ~999nm and in Fig 4 (d) at the longer wavelength side ~1007nm, using the same wavelength span. At this power, the SMD is ~3% at the central wavelength and ~20% at the longer wavelength where, as for the tilted facet SLDs described above, Joule heating causes a shift of the emission spectrum which results in the window becoming transparent to these longer wavelengths. This is further evidenced by the period of the spectral modulation, which is 0.064nm at ~999nm but 0.126nm at longer wavelengths. This is consistent with a change in the dominant feedback cavity from reflection at the stripe/window interface to reflection from the cleaved back facet after transmission through the window, which occurs at longer wavelength. <10% SMD was measured for an output power of 10mW. Improvement in heatsinking could be expected to reduce the SMD, allowing higher powers to be achieved with lower SMD. Figure 4 (e) and (f) show the optical far-field [3D] topography recorded at 350mA from tilted and normal facet SLDs respectively. Whilst the profile for the tilted SLD is crescent-shaped, that for the normal-to-facet SLD takes the expected elliptical form of a normal waveguide, with 41.4° fast-axis and 4.6° slow-axis divergence.

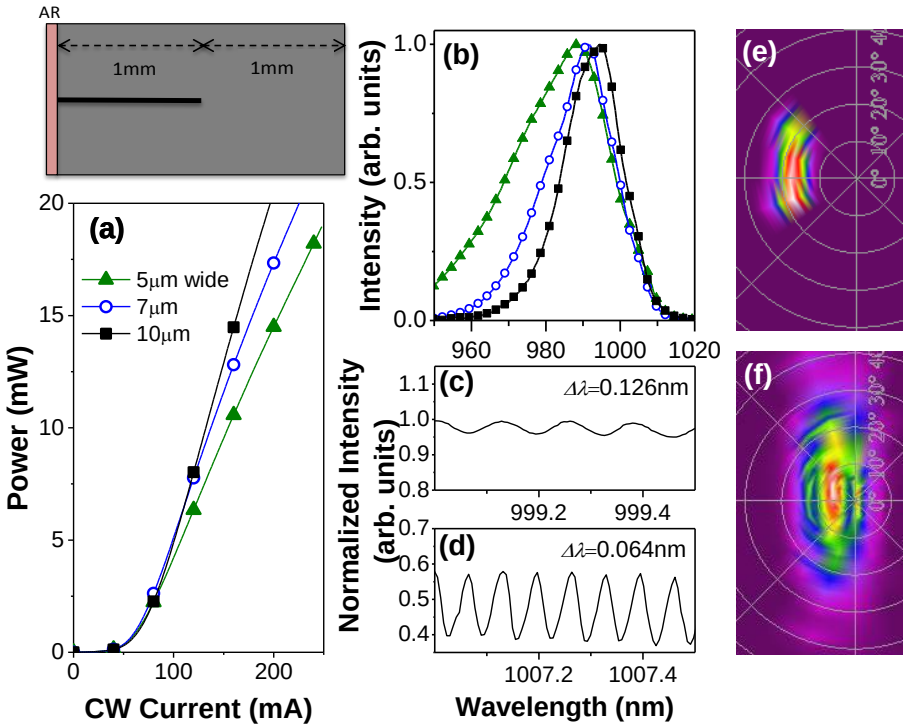

Figure 4. Performance of 1mm long self-aligned stripe SLD with 1mm long window. (a) Power as a function of current density for 5, 7 and 10μm wide stripes. (b) Normalized low resolution EL spectra recorded at 20mW output power. (c) and (d) show the normalized high resolution EL spectrum of the 10μm wide SLD plotted over reduced ranges for the central peak, (c), and the long wavelength region, (d). The far-field profile is shown for a tilted facet SLD, (e) and the normal-to-facet SLD at 350mA

At this point in time, commercially available SLDs based on similar active widths demonstrate similar performance (power and spectral modulation) to that reported here. Our approach therefore offers comparable performance, but avoids the need for application of AR coatings, which will be beneficial in the pursuit of broader bandwidth SLDs. Alternatively, ultra-low ripple is also possible via application of specialist multi-layer facet coatings in conjunction with our window-like facets.

CONCLUSIONS

We have demonstrated GaAs-based SLDs based on a self-aligned stripe process with incorporation of a naturally broadband window-like back facet for attainment of low R_{eff} over a broad bandwidth, without the need for application of facet coatings. This has resulted in the realization of high power (>30mW) and low SMD (<5%) CW SLDs. The relation between SMD, power, and stripe length has been investigated, building the design criteria for high power and low SMD SLDs. Joule-heating in the CW-pumped SLD stripes results in a deviation from the fit to the SMD *versus* output power curve, shifting the gain region relative to the unpumped absorbing window. Furthermore, SLDs processed normal to the facet demonstrate CW output powers as high as 20mW, offering improvements in beam quality, ease of packaging and use of material real estate compared to those based on the traditional tilted waveguide.

ACKNOWLEDGEMENTS

The authors gratefully acknowledge research grants provided by the UK Engineering & Physical Sciences Research Council (EPSRC), references EP/J004898/1 and EP/I018328/1.

REFERENCES

[1] Profio, A. E. and Doiron, D. R., "Transport of light in tissue in photodynamic therapy of cancer", Photochem. Photobiol. 46, p.591, 1987.
[2] Drexler, W., Fujimoto, J., Optical coherence tomography: Technology and Application, Springer-Verlag (2008).
[3] Cha, I., Kitamura, M., Mito, I., "1.5μm band travelling-wave semiconductor optical amplifiers with window facet structure," Electronics Letters 25 (3), 242 (1989)
[4] Connelly, M. J., Semiconductor Optical Amplifiers, Klewer Academic Publishers (2004).
[5] Fu, L., Schweizer, H., Zhang, Y., Li, L., Baechle, A., Jochum, S., Bernatz, G. C., and Hansmann, S., "Design and Realization of High-Power Ripple-Free Superluminescent Diodes at 1300nm". IEEE J. Quant. Elec. 40 (9), p. 1270, 2004.
[6] Nagai, H., Noguchi, Y., Sudo, S., "High-Power, high-efficiency 1.3μm superluminescent diode with a buried bent absorbing guide structure", Appl. Phys. Lett. 54 (16), p.1719, 1989.
[7] Semenov, A. T., Shidlovski, V. R., Safin, S. A., Konyaev, V. P., Zverkov, M. V., "Superluminescent diodes for visible (670nm) spectral range based on AlGaInP/GaInP heterostructures with tapered grounded absorber", Electronics. Letters, 29 (6), p.530, 1993.
[8] Burrow, L., Causa, F., Sharma, J., "Ripple-free superluminescent diode". IEEE Photonics Technology Letters, 17 (10), pp.2035-37, 2005
[9] Kashima, Y., Matoba, A., Takano, H., "Performance and reliability of InGaAsP superluminescent diode". Journal of Lightwave Technology, 10 (11), pp.1644-1649, 1992.
[10] Matsumoto, M., Sasaki, K., Kondo, M., Ishizumi, T., Takeoka, T., Nakatsu, H., Watanabe, M., Yamamoto, O., and Yamamoto, S., "High-power 780 nm AlGaAs narrow-stripe window structure lasers with window grown on facets", Jpn. J. Appl. Phys., 32, pp.665 -667 1993
[11] Kwong, N. S. K., Lau, K. Y., Bar-Chaim, N., "High-Power High-Efficiency GaAlAs Superluminescent Diodes with an Internal Absorber for Lasing Suppression", IEEE Journal of Quantum Electronics, 25 (4), pp.696-704, 1989.
[12] Tateoka, K., Naito, H., Yuri, M., Kume, M., Hamada, K., Shimizu, H.,Kazumura, M., Teramoto, I., "A High-Power GaAlAs Superluminescent Diode with an Antireflective Window Structure". IEEE J. of Quan. Elect. 27 (6), pp 1568-1573, 1991.
[13] Groom, K. M., Alexander, R. R., Childs, D. T. D., Krysa, A. B., Roberts, J. S., Helmy, A. S., Hogg, R. A., "GaAs-Based Self-Aligned Laser Incorporating InGaP Opto-Electronic Confinement Layer" Electronics Letters, 44 (15), pp.905-6, July 2008
[14] Zhang, Z. Y., Luxmoore, I. J., Jiang, Q., Liu, H. Y., Groom, K. M., Childs, D. T., Hopkinson, M., Cullis, A. G., and Hogg, R. A., "Broadband quantum dot superluminescent LED with angled facet formed by focused ion beam etching", Electron. Lett. 43, 587, (2007).
[15] Vasil'ev, P, Ultrafast Diode Lasers, Fundamentals and Applications, 1995, Artech House.
[16] Suhara, T, "Semiconductor Laser Fundamentals", 2004, New York: Marcel Dekker.
[17] Zhang, Z. Y., Wang, Z. G., Xu, B., Jin, P., Sun, Z. Z., and Liu, F. Q., "High-Performance Quantum-Dot Superluminescent Diodes", IEEE Phot. Tech. Lett. 16, (1), p.27, 2004
[18] Hakki, B. W. and Paoli, T. L., "Gain spectra in GaAs double-heterostructure injection lasers". Journal of Applied Physics, 46, (1299), 1975